Vortex Evolution and Bound Pair Formation in Anisotropic Nonlinear Optical Media

A. V. Mamaev,[1] M. Saffman,[2] and A. A. Zozulya[3]
[1]*Institute for Problems in Mechanics, Russian Academy of Sciences, Prospekt Vernadskogo 101, Moscow, 117526 Russia*
[2]*Department of Optics and Fluid Dynamics, Risø National Laboratory, Postbox 49, DK-4000 Roskilde, Denmark*
[3]*JILA, University of Colorado, Campus Box 440, Boulder, Colorado 80309-0440*
(Received 25 July 1996)

We present a theoretical and experimental study of the propagation, decay, and interaction of optical vortices in media with an anisotropic nonlocal nonlinearity. The initial stage of decay of a circular vortex is characterized by charge dependent rotation, and stretching of the vortex. Our results suggest that a compact vortex of unit topological charge cannot exist in such media, but that a counterrotating vortex pair can form a bound state. Some analogies and differences between optical vortices and the classical dynamics of vortices in an ideal fluid are described. [S0031-9007(96)01742-5]

PACS numbers: 42.65.Tg, 42.65.Hw, 42.65.Sf, 47.32.Cc

Vortex solitons exist in media with a defocusing nonlinearity. Their stability depends on the structure of the nonlinearity and the dimensionality of the medium. Evolution in a medium with cubic nonlinearity in the limit of one transverse dimension is described by the $(1 + 1)$D nonlinear Schrödinger equation which is integrable, and admits solitary wave solutions both for focusing and defocusing nonlinearities [1]. Planar $(1 + 1)$D solutions are modulationally unstable in bulk media described by a $(2 + 1)$D system of equations. This was known theoretically at an early stage [2–4], and has been seen experimentally in water waves [5] and in nonlinear optics both in atomic vapors with a Kerr type response [6] and in photorefractive media [7]. Three dimensional solitary vortex solutions of the nonlinear Schrödinger equation were first considered in the context of superfluidity [8] and have attracted a great deal of recent interest in nonlinear optics [9]. Kerr type optical media with a cubic, isotropic, and local nonlinearity support $(1 + 1)$D vortex solitons [10].

A Kerr type nonlinearity is, however, a simplified idealized model of a nonlinear response. The evolution of vortices in media with a more complex nonlinear response has not been studied extensively. The bulk photorefractive nonlinear medium used in the experiments reported here exhibits a nonlinearity that is both anisotropic and nonlocal. This leads to some remarkable qualitative differences in the spatial dynamics of light beams. In particular an optical vortex with initial circular symmetry rotates and stretches, aligning itself so that its major axis coincides with the direction of greatest material nonlinearity. The stretching proceeds unchecked so that the vortex becomes more and more delocalized. Both theory and experiment indicate that, in contradiction to results reported earlier [11], localized optical vortex solutions and, in particular, soliton vortex solutions of unit topological charge do not exist in these media. The nonexistence of localized vortex solutions is not a simple consequence of the anisotropy alone since, in related work done in the same material but with a self-focusing nonlinearity, we have demonstrated convergence to elliptical soliton solutions [12].

Despite the above unique features of spatial dynamics of single vortices the initial development of beams with several embedded vortices demonstrates spatial dynamics reminiscent of that known from the classical theory of point vortices in fluids [13] and superfluids [14]. This is not unexpected since there is a close mathematical analogy between the nonlinear Schrödinger equation and the mechanics of fluids in two dimensions [8,15]. The spatial evolution of the optical field $B(\vec{r})$ is described in dimensionless form by the equation

$$\left(\frac{\partial}{\partial x} - \frac{i}{2}\nabla^2\right)B(\vec{r}) = -i\hat{f}(|B|^2)B(\vec{r}). \qquad (1)$$

The differential operator $\nabla = \hat{y}\partial/\partial y + \hat{z}\partial/\partial z$ acts on coordinates y and z perpendicular to the direction of propagation of the beam x, and the operator $\hat{f}(|B|^2)$ describes the nonlinearity [see Eq. (4)]. Time evolution is replaced here by propagation along the coordinate x. Writing the optical field in the form $B = \sqrt{\rho}\, e^{\iota\psi}$, we obtain the continuity equation

$$\rho_x + \nabla \cdot (\rho\vec{v}) = 0, \qquad (2)$$

where ρ is the density and $\vec{v} = \nabla\psi$ is identified as the velocity, together with the Euler equation for the velocity field

$$\vec{v}_x + \vec{v} \cdot \nabla\vec{v} = \nabla\left(-\hat{f} + \frac{\nabla^2\sqrt{\rho}}{2\sqrt{\rho}}\right). \qquad (3)$$

Equations (2) and (3) are valid where the velocity field is irrotational away from the zeros of ρ. In Kerr media $\hat{f} = \rho$ and the pressure is given by $p = \rho^2/2$, while the last term on the right hand side of (3) is a nonlinear correction to the pressure. In the photorefractive media considered here the material response is anisotropic and is given by [16] $\hat{f} = \alpha\,\partial\phi/\partial z$, where the electrostatic potential ϕ satisfies

$$\nabla^2\phi + \nabla\ln(1 + |B|^2) \cdot \nabla\phi = \frac{\partial}{\partial z}\ln(1 + |B|^2). \qquad (4)$$

The nonlinearity coefficient α is proportional to the amplitude of an externally applied electric field: $\alpha \propto E_{\rm ext}$ (for details see [7,16]). The pressure is therefore anisotropic which results in a straining flow, with the largest principal component along the z coordinate. Note that for a $(2+1)$D beam the nonlinearity (4) never becomes isotropic. The degree of anisotropy as measured by the ratio of focal lengths of the nonlinear lens along the z and y coordinates induced by a round beam is equal to three, regardless of the level of the applied voltage or the saturation intensity. This fact for the self-focusing case was established in Refs. [16,17], and confirmed experimentally in Ref. [17]. It is equally true for the defocusing case since the structure of Eq. (4) does not change.

It has been shown [18] that for large intervortex separation the dynamics of vortices satisfying the cubic nonlinear Schrödinger equation correspond to point vortex dynamics in a fluid. The particular structure of Eq. (4) leads here to more complex dynamics. For small initial separation a pair of counter-rotating vortices annihilate, as is the case under linear evolution in free space. At larger initial separations they form a bound pair, aligned perpendicular to z, that corresponds to the steadily translating counterrotating vortex pair in fluids. Anisotropy of the nonlinearity results in alignment of the bound pair perpendicular to the z axis, irrespective of the direction of their initial separation. Although we can say nothing definite about the asymptotic stability, the nonlinearity prevents the annihilation seen in linear propagation, and arrests the stretching seen in the propagation of a single vortex at distances and nonlinearities analyzed in the theory and the experiment.

The experimental arrangement was similar to that used in Ref. [7]. A 30 mW He-Ne laser beam ($\lambda = 0.63\ \mu$m) was passed through a variable beam splitter and a system of lenses controlling the size of the beam waist. The beam was directed into a photorefractive crystal of SBN:60 doped with 0.002% by weight Ce. The beam propagated perpendicular to the crystal $\hat{c}$ axis ($= z$ axis), and was polarized along it. The crystal measured 19 mm along the direction of propagation, and was 5 mm wide along the $\hat{c}$ axis. A variable dc voltage was applied along the $\hat{c}$ axis to control the value of the nonlinearity coefficient α. Images of the beam at the output face of the crystal were recorded with a CCD camera. Beams with embedded vortex structures were produced with the help of computer-generated holograms corresponding to the interference pattern created by the target structure of the field (a single or a set of vortices) and a plane reference beam. Diffraction of the laser beam by the hologram read out the target structure and embedded it in the beam.

Figure 1 shows evolution of a single charge-one vortex after propagating through the nonlinear medium for different values of the nonlinearity. Input boundary conditions corresponded to a vortex embedded in a Gaussian beam creating an annular ring with about 10 and 36 μm internal and external diameters, respectively. The normalized maximum intensity of the light field was of the order of the saturation intensity $|B_{\max}|^2 \approx 1$.

Linear propagation of the input field through the crystal resulted in diffractive spreading producing an annular ring with about 76 and 270 μm internal and external diameters, respectively [Fig. 1(a)]. The frame on the right of Fig. 1(a) shows the interference pattern of this output field with a spherical reference wave. A single spiral originating in the center of the beam and unwinding outward is a signature of a charge-one vortex embedded in the beam (cf. [19]). Increasing the nonlinearity (applied voltage) in Figs. 1(b)–1(d) results in focusing of the vortex perpendicular to the z axis, stretching along the z axis, and rotation. The redistribution of the field creates an intensity dip along the z axis; the field from the dip is pushed out along the positive and negative y axis forming two lobes. The alignment and stretching along z is to some degree analogous to the elongation of an elliptical vortex patch in a straining field [13]. The analogy with a vortex patch is, however, incomplete since $\vec{v} = \nabla\psi$ implies that we are dealing with point vortices.

The observed rotation of the vortex away from the z axis is due to the fact that the nonlinearity generates harmonics with high azimuthal indices. These harmonics have different phase velocities resulting in relative phase

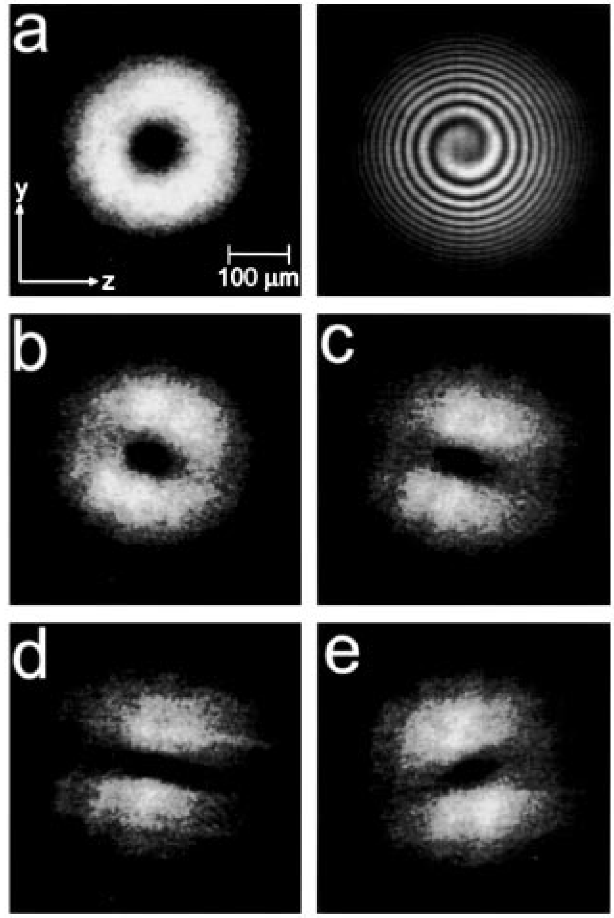

FIG. 1. Evolution of a charge-one vortex for applied voltages of (a) 0, (b) 200, (c) 400, and (d) 800 V. Frame (e) is analogous to (c) but for the opposite vortex sign. The frame to the right of (a) is the interference pattern of the output field (a) and a spherical reference wave.

shifts and rotation of the vortex as a whole. The anisotropy of the nonlinearity counterbalances the rotation and stops it with the major axis of the vortex ellipsoid oriented at a small angle to the z axis. Since the direction of rotation is uniquely determined by the vortex charge changing its sign results in mirror reflection of the whole picture with respect to the z axis as is shown in Fig. 1(e), obtained for the same parameters as Fig. 1(c), but with the opposite vortex charge.

Figure 2 presents the results of a numerical solution of Eqs. (1) and (4) for the experimental parameters of Fig. 1 and demonstrates quite good agreement with experimental data. Besides the case of a vortex embedded in a Gaussian beam (as in our experiments) the numerical analysis has been carried out with the vortex put on an infinite plane wave background. Typical vortex dynamics for this case are shown in Fig. 3. The solution is presented in the dimensionless coordinates of Eqs. (1) and (4), the nonlinearity is fixed at the level $|B(\infty)| = 1$ and Figs. 3(a)–3(d) correspond to increasing values of the normalized propagation coordinate changing from 0 to 30 in increments of 10. For typical experimental parameters this propagation length exceeds the characteristic size of photorefractive media several times. The initial vortex diameter equals 10 in dimensionless units [7].

In all cases the vortex evolution was characterized by continuous spreading along the z direction, thereby confirming that the experimentally observed dynamics are intrinsic to the vortex structure of the field and are not changed qualitatively by the dynamics of the embedding Gaussian beam. Initial stages of vortex evolution are accompanied in all cases by the generation of radiating waves originating at the vortex core and propagating outward. These waves are especially noticeable in the case of a vortex on an infinite background (see Fig. 3). Nonlinear evolution of the field in this case generates two high-intensity lobes around the vortex core aligned primarily along the y axis at a small angle to it. These lobes are similar to those seen in Figs. 1 and 2.

Figure 4 shows the dynamics of a counterrotating pair of charge-one vortices with opposite signs. Input boundary conditions corresponded to a closely spaced pair of vortices with opposite topological charges placed in the center of a Gaussian beam and arranged perpendicular to the direction of the externally applied electric field (z axis). The lower vortex rotated clockwise and the upper one counterclockwise. The input diameter of the Gaussian carrier was about 180 μm, the diameter of each vortex 33 μm, and they were about 20 μm apart. In the absence of nonlinearity oppositely charged vortices coalesce and annihilate due to diffraction. The linear diffraction pattern of the annihilated pair is a crescent-shaped dip of intensity that spreads out and moves from the center of the beam to the right, as shown in Fig. 4(a). Scans of the beam profile in Fig. 4(a) and interferometric measurements show that the intensity at the bottom of the crescent does not reach zero.

Nonlinearity arrests diffraction-driven annihilation and allows the pair of vortices to form a nonlinear bound state as is seen in Figs. 4(b) and 4(c) taken at 550 and 770 V external voltage, respectively. Interferometric measurements confirm the presence of two separate vortices in both Figs. 4(b) and 4(c). Figures 4(d) and 4(f) are theoretical calculations corresponding to the experimental Figs. 4(a)–4(c), respectively. Note the motion of the vortex pair to the right in Figs. 4(e) and 4(f). It is analogous

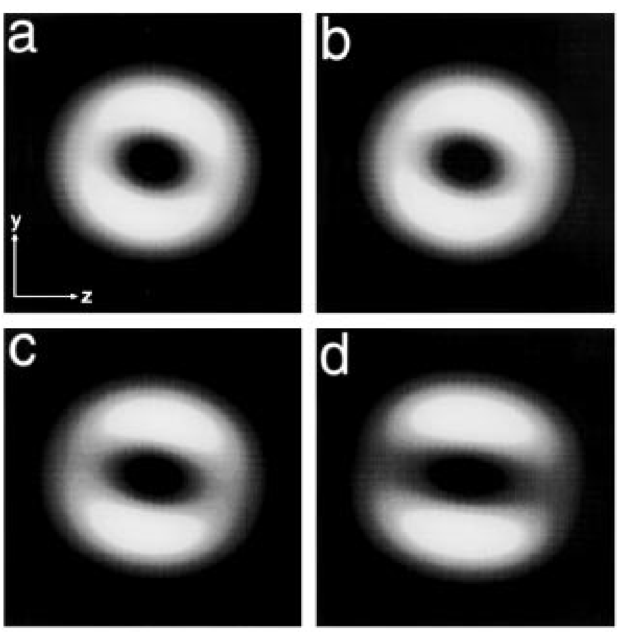

FIG. 2. Numerical results corresponding to parameters of Fig. 1. The applied voltages are (a) 0, (b) 200, (c) 400, and (d) 800 V.

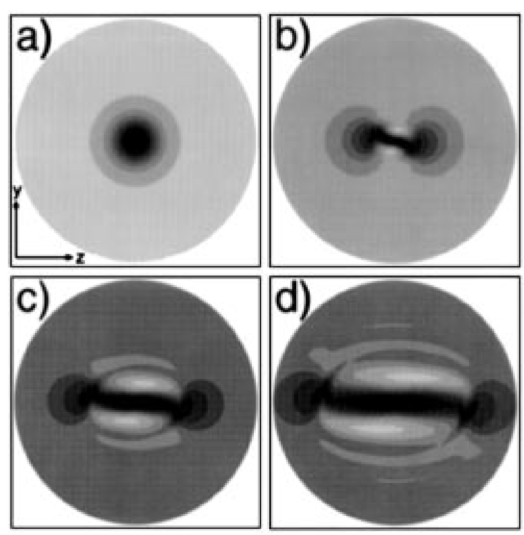

FIG. 3. Typical numerical results showing vortex dynamics on a plane wave background. The initial vortex diameter equals $d = 10$ and $|B_\infty| = 1$. The propagation distances are (a) 0, (b) 10, (c) 20, and (d) 30 V.

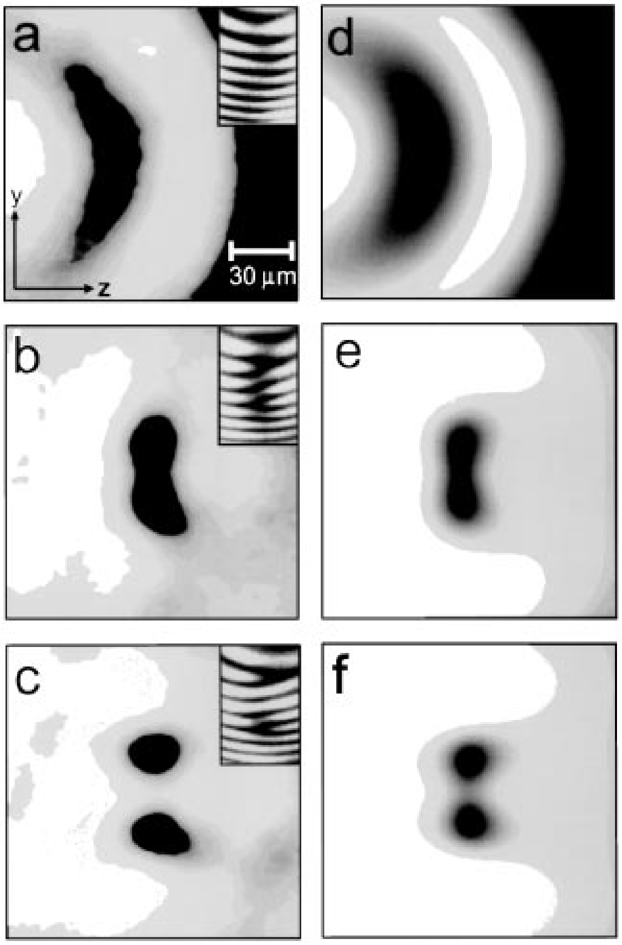

FIG. 4. Evolution of a pair of oppositely charged vortices for applied voltages of (a),(d) 0, (b),(e) 550, and (c),(f) 770 V. Frames (a)–(c) are experiment, (d)–(f) theory. Insets in frames (a)–(c) are interferometric pictures verifying the existence [nonexistence for frame (a)] and localization of vortices.

to the translational motion of a point vortex pair in fluid dynamics [13]. Because of the highly anisotropic character of the nonlinear response (4) the orientation of the pair is crucial for its subsequent evolution. The same vortex pair aligned along the direction of the applied field (z axis) tends to coalesce and annihilate, even for nonzero nonlinearity. Both experimental data and numerics indicate robustness of the vortex pair configuration that is aligned perpendicular to the z axis. Thus a vortex pair placed at an angle to the z axis tends to realign itself perpendicular to the z axis to counterbalance diffraction by the nonlinearity. The question of asymptotic existence and stability of bound vortex pairs remains open.

In summary, we have studied vortex dynamics in nonlocal anisotropic nonlinear optical media. Some features of the dynamics are related closely to point vortex dynamics in fluids, but the different form of nonlinearity results in qualitatively different phenomena. The vortex dynamics are characterized by prominent anisotropy-induced stretching and alignment effects. Numerical results based on a three dimensional model are in close agreement with the observed dynamics.

We are grateful to E. Eilertsen and E. Rasmussen for preparing the holographic masks. This work was supported by the Danish Natural Science Research Council. A. A. Z. acknowledges the support of the U.S. National Science Foundation Optoelectronics Computing Center, an NSF Engineering Research Center.

[1] V. E. Zakharov and A. B. Shabat, Zh. Eksp. Teor. Fiz. **61**, 118 (1971) [Sov. Phys. JETP **34**, 62 (1972)]; V. E. Zakharov and A. B. Shabat, Zh. Eksp. Teor. Fiz. **64**, 1627 (1973) [Sov. Phys. JETP **37**, 823 (1973)].
[2] V. E. Zakharov and A. M. Rubenchik, Zh. Eksp. Teor. Fiz. **65**, 997 (1973) [Sov. Phys. JETP **38**, 494 (1974)].
[3] E. A. Kuznetsov and S. K. Turitsyn, Zh. Eksp. Teor. Fiz. **94**, 119 (1988) [Sov. Phys. JETP **67**, 1583 (1988)].
[4] G. S. McDonald, K. S. Syed, and W. J. Firth, Opt. Commun. **95**, 281 (1993); C. T. Law and G. A. Swartzlander, Jr., Opt. Lett. **18**, 586 (1993).
[5] E. D. Brown *et al.*, J. Fluid Mech. **204**, 263 (1989).
[6] V. Tikhonenko, J. Christou, B. Luther-Davies, and Y. S. Kivshar, Opt. Lett. **21**, 1129 (1996).
[7] A. V. Mamaev, M. Saffman, and A. A. Zozulya, Phys. Rev. Lett. **76**, 2262 (1996); A. V. Mamaev, M. Saffman, and A. A. Zozulya, Europhys. Lett. **35**, 25 (1996); A. V. Mamaev, M. Saffman, D. Z. Anderson, and A. A. Zozulya, Phys. Rev. A **54**, 870 (1996).
[8] V. L. Ginzburg and L. P. Pitaevskii, Zh. Eksp. Teor. Fiz. **34**, 1240 (1958) [Sov. Phys. JETP **34**, 858 (1958)].
[9] Yu S. Kivshar, IEEE J. Quantum Electron. **28**, 250 (1993); G. S. McDonald, K. S. Syed, and W. J. Firth, Opt. Commun. **94**, 469 (1992); K. Staliunas, Chaos Solitons Fractals **4**, 1783 (1994).
[10] G. A. Swartzlander, Jr. and C. T. Law, Phys. Rev. Lett. **69**, 2503 (1992).
[11] G. Duree *et al.*, Phys. Rev. Lett. **74**, 1978 (1995).
[12] A. A. Zozulya, D. Z. Anderson, A. V. Mamaev, and M. Saffman, Europhys. Lett. (to be published).
[13] P. G. Saffman, *Vortex Dynamics* (Cambridge University Press, Cambridge, 1992).
[14] E. B. Sonin, Rev. Mod. Phys. **59**, 87 (1987).
[15] E. A. Spiegel, Physica (Amsterdam) **1D**, 236 (1980).
[16] A. A. Zozulya and D. Z. Anderson, Phys. Rev. A **51**, 1520 (1995).
[17] N. Korneev *et al.*, J. Mod. Opt. **43**, 311 (1996).
[18] A. L. Fetter, Phys. Rev. **151**, 100 (1966); F. Lund, Phys. Lett. A **159**, 245 (1991).
[19] I. V. Basistiy, V. Yu. Bazhenov, M. S. Soskin, and M. V. Vasnetsov, Opt. Commun. **103**, 422 (1993).